Changes in Actin Structural Transitions Associated with Oxidative Inhibition of Muscle Contraction†

Ewa Prochniewicz, Daniel Spakowicz, and David D. Thomas*

Department of Biochemistry, Molecular Biology, and Biophysics, University of Minnesota, Minneapolis, Minnesota 55455

Received June 7, 2008; Revised Manuscript Received July 29, 2008

ABSTRACT: We have used transient phosphorescence anisotropy (TPA) to detect changes in actin structural dynamics associated with oxidative inhibition of muscle contraction. Contractility of skinned rabbit psoas muscle fibers was inhibited by treatment with 50 mM H_2O_2, which induced oxidative modifications in the myosin head and in actin, as previously reported. Using proteins purified from oxidized and unoxidized muscle, we used TPA to measure the effects of weakly (+ATP) and strongly (no ATP) bound myosin heads (S1) on the microsecond dynamics of actin labeled at Cys374 with erythrosine iodoacetamide. Oxidative modification of S1 had no effect on actin dynamics in the absence of ATP (strong binding complex), but restricted the dynamics in the presence of ATP (weakly bound complex). In contrast, oxidative modification of actin did not have a significant effect on the weak-to-strong transitions. Thus, we concluded that (1) the effects of oxidation on the dynamics of actin in the actomyosin complex are predominantly determined by oxidation-induced changes in S1, and (2) changes in weak-to-strong structural transitions in actin and myosin are coupled to each other and are associated with oxidative inhibition of muscle contractility.

Structural Transitions in Actin and Myosin during the Actomyosin ATPase Cycle. Current models of the molecular mechanism of muscle contraction propose that force is generated during the transition of the actin−myosin complex from states of weak binding (with ATP bound to myosin) to states of strong binding (with ADP or no nucleotide bound to myosin). Spectroscopic studies on the dynamics of myosin in this cycle have been inspired by the classical "rotating crossbridge" hypothesis and led to the conclusion that force is generated by a transition of the myosin head from a disordered, weakly bound state to an ordered, strongly bound state (*1*−*3*). This transition has functional relevance, since changes in the distribution between these two myosin structural states have provided a molecular explanation for age-related decline in skeletal muscle force generation (*4, 5*).

The weak-to-strong structural transition in myosin has inspired research on the structural states of myosin-bound actin. Measurements of steady-state phosphorescence anisotropy (*6*), bending motions of actin filaments (*7*), and polarized fluorescence of actin in muscle fibers (*8, 9*) showed that strong and weak myosin binding have different effects on the structure and dynamics of the actin filament, providing early support for the hypothesis that actin undergoes weak-to-strong structural transitions in parallel to myosin.

Our previous studies established transient phosphorescence anisotropy (TPA) as a powerful method for analyzing the coupling between structural dynamics of actin and myosin. Quantitative analysis of the intrafilament rotational dynamics of actin (*10*) showed that strong binding of myosin causes highly cooperative changes in actin dynamics (*11*), while weak binding of myosin produces a new structural state, intermediate between that of strongly bound and free actin (*12*). We concluded that transitions in the dynamics of actin parallel transitions in the dynamics of interacting myosin heads, and that the generation of force and movement by actomyosin requires that both proteins undergo a weak-to-strong structural transition. This conclusion led to the hypothesis that structural transitions in actin, as in myosin, have functional relevance; this hypothesis predicts that perturbation of muscle contractility is associated with perturbation of the weak-to-strong transition in both proteins, and this hypothesis is tested in the present study.

Perturbation of Muscle Contractility by Hydrogen Peroxide Treatment. Hydrogen peroxide treatment of skinned muscle fibers serves as a model for the modifications in protein structure and function that occur under oxidative stress, as in aging or disease (*5*). The effects of hydrogen peroxide treatment of muscle on mechanical and enzymatic function were described in our previous study (*13*), which showed that a 30-min treatment of skinned rabbit psoas muscle fibers with 50 mM H_2O_2 significantly decreased isometric force and myofibrillar ATPase activity, and completely inhibited shortening. The studies on the molecular basis of these effects were focused on changes in myosin. Mass spectrometry detected oxidation of multiple sites in the heavy and light chains of the myosin head, and electron paramagnetic resonance measurements of fibers in rigor, relaxation, and contraction showed that peroxide treatment increased the fraction of myosin heads in the rigor-like

† This work was supported by grants to D.D.T. from NIH (AR32961 and AG26160) and the University of Minnesota Biomedical Genomics Center.

* Address correspondence to this author: Dept. of Biochemistry, Molecular Biology, and Biophysics, University of Minnesota, Jackson Hall 6-155, 321 Church St., Minneapolis, MN 55455. Tel: (612) 625-0957. Fax: (612) 624-0632. E-mail: ddt@umn.edu.

10.1021/bi801080x CCC: $40.75
Published on Web 10/15/2008

structural state, with resulting force production, under conditions that would normally produce relaxation. We concluded that peroxide-induced perturbation of muscle function is associated with oxidation-induced decrease in the extent of the weak-to-strong transition in myosin. The goal of the present work is to test the role of structural transitions in actin in peroxide-induced perturbation of muscle function. We purified actin and myosin from unoxidized and oxidized muscle fibers, attached a phosphorescent dye to actin, then used TPA to determine the effects of myosin and/or actin oxidation on the microsecond rotational dynamics of actin.

MATERIALS AND METHODS

Preparation and Oxidation of Skinned Muscle Fiber Bundles. Skinned muscle fibers were prepared from rabbit psoas muscle, permeabilized and oxidized as described previously (*13*). Briefly, strips of psoas muscle were freshly dissected from New Zealand white rabbits and skinned (permeabilized) by incubating the strips for 6 h at 4 °C on a shaker in a glycerination buffer (60 mM potassium propionate, 25 mM MOPS pH 7.0, 2 mM $MgCl_2$, 9 mM EGTA, 1 mM NaN_3, 0.5% Triton X100, 25% glycerol). Strips were then incubated for 20 h in a storage buffer (60 mM potassium propionate, 25 mM MOPS pH 7.0, 2 mM gCl_2, 1 mM EGTA, 1 mM NaN_3, 50% glycerol) at 4 °C and finally transferred to fresh storage buffer containing 0.1 mM DTT and stored at −20 °C for up to 5 months. Skinned strips were further dissected on ice into 0.5−1 mm thick fiber bundles, collected in a 50 mL Falcon tube and glycerol was washed out by three cycles of 2 min centrifugation at 1800*g* and resuspension of pelleted fiber bundles in rigor buffer (RB: 130 mM potassium propionate, 25 mM MOPS pH 7.0, 6 mM $MgCl_2$, 1 mM EGTA) at 4 °C. The final suspension of skinned fiber bundles was divided, and one part was designated for a control, unoxidized sample and the other part was designated for oxidation. Oxidation was carried out by incubating fiber bundles for 30 min at 25 °C in RB containing 50 mM H_2O_2. To terminate oxidation, H_2O_2 was washed out by two cycles of 2 min centrifugation at 1800*g* and resuspension of pelleted fibers in RB at 4 °C. Washed fiber bundles were then reduced by 15 min incubation at 4 °C in RB supplemented by 10 mM DTT. Reduced fiber bundles were washed five times at 4 °C in 20 mM Tris pH 7.5 and used for purification of actin and myosin. Control unoxidized samples were always prepared and treated in parallel to the oxidized samples except for the omission of H_2O_2.

Protein Preparations. Myosin S1 and actin were prepared as described previously, either from bulk rabbit back and leg muscles (*12*) or from skinned rabbit psoas fiber bundles (*13*). To determine the effects of oxidation, we measured the interaction of fiber proteins (either S1 or actin from oxidized and unoxidized fiber bundles) with bulk muscle proteins (either actin or S1, respectively). For simplicity, the proteins prepared from bulk rabbit muscle are referred to as "S1" or "actin", while the proteins prepared from oxidized and unoxidized fiber bundles are referred to as "oxidized" or "unoxidized" S1 or actin.

Two independent preparations of unoxidized−oxidized pairs of S1 and four independent preparations of unoxidized−oxidized pairs of actin were used. Labeling of actin at Cys 374 with ErIA (AnaSpec) was performed as described previously (*12*). Actin (48 μM) was polymerized with 2 mM $MgCl_2$ in 20 mM Tris (pH 7.5), and ErIA, freshly dissolved in DMF, was added at a concentration of 480 μM. After 2 h incubation at 25 °C, labeling was stopped by 10 mM DTT, actin was ultracentrifuged 1 h at 200000*g*, pellets were suspended in Mg-G-buffer (5 mM Tris pH 7.5, 0.2 mM $MgCl_2$, 0.5 mM ATP), clarified by 10 min centrifugation at 300000*g*, and actin was polymerized for 30 min at 25 °C by adding 2 mM $MgCl_2$. After ultracentrifugation for 1 h at 200000*g*, pellets were suspended in Mg-F-buffer (3 mM $MgCl_2$, 10 mM Tris, pH 7.5) containing 0.2 mM ATP, and the labeled F-actin was immediately stabilized against depolymerization and denaturation by adding 1 molar equiv of phalloidin. The extent of labeling (mol of dye/mol of actin), determined by measuring absorbance of labeled actin at 538 nm, was in the range of 0.75 to 0.97.

The concentration of purified unlabeled actin and S1 was measured by ultraviolet absorption, assuming molar extinction coefficients of 0.63 mg mL^{-1} cm^{-1} for actin at 290 nm and 0.75 mg mL^{-1} cm^{-1} for S1 at 280 nm. Concentration of labeled actin was measured by the Bradford protein assay (*14*) (BioRad) using unlabeled actin of known concentration as a standard.

TPA Experiments. Phalloidin-stabilized ErIA-F-actin was diluted in Mg-F-buffer to 1.2 μM, and acto-S1 complexes were formed by adding 0.12−5 μM S1, as indicated in the text. To prevent photobleaching of the dye during TPA measurement, oxygen was removed from the sample by 5 min incubation with glucose oxidase (55 μg/mL), catalase (36 μg/mL), and glucose (45 μg/mL) (*12*). Phosphorescence was measured at 25 °C as described previously (*10*) with slight modification of the TPA spectrometer. The actin-bound ErIA was excited with a vertically polarized 10-ns pulse from a XeCl-pumped (Compex 120, Lambda Physics) dye laser at 540 nm, using 5 mM coumarin 548 in ethanol, operating at a repetition rate of 100 Hz. Phosphorescence emission was extracted by a 670 nm long-pass glass cutoff filter (Corion), then detected by a photomultiplier (R928, Hamamatsu), and digitized by transient digitizer (CompuScope 14100, GaGe) using a time resolution of 1 μs/channel. The time-resolved phosphorescence anisotropy decay was calculated according to

$$r(t) = [I_v(t) - GI_h(t)]/[I_v(t) + 2GI_h(t)] \quad (1)$$

where $I_v(t)$ and $I_h(t)$ are vertically and horizontally polarized components of the emission signal. These components were detected at 90° with a single detector and a Polaroid sheet polarizer that alternates between two orientations every 500 laser pulses. G is an instrumental correction factor, determined by performing the measurement with horizontally polarized excitation, for which the corrected anisotropy value is set to zero. The time-dependent anisotropy decays of free actin and strongly bound complexes with S1 were obtained by recording 10 cycles of 1000 pulses (500 in each orientation of the polarizer), corresponding to a total acquisition time of about 2 min. To analyze weakly bound complexes, ATP (3 mM) was added directly to the cuvette containing a strongly bound complex (2.5 μM or 5 μM S1), the sample was gently mixed, and measurements started 10−15 s later. To ensure that these data sets were acquired in the presence of saturating ATP, a sequence of brief

acquisitions (about 30 s each) was performed to confirm that a stable steady state was reached (*12*). $I_v(t)$ and $I_h(t)$ from several samples were typically averaged to minimize noise.

TPA Data Analysis. Final anisotropy was defined as the average value of r_F in the time window from 400 to 500 μs, which has been shown previously to provide the most sensitive and precise measurement of actin's microsecond rotational dynamics (*11*). The effect of strongly bound S1 on the final anisotropy of actin was further analyzed in terms of the linear lattice model (eq 2) as in our previous work (*15*), assuming that perturbation of one protomer in an actin filament affects a segment containing N protomers:

$$r_F = r_{Fmax} - (r_{Fmax} - r_{Fmin})(1 - x)^N \quad (2)$$

where r_{Fmin} and r_{Fmax} are the limiting values at 0 and infinite S1, and x = [S1]/[actin protomer]. The adjustable parameters in the least-squares fit were r_{Fmax} and N.

To determine the effect of strongly and weakly bound S1 on rotational correlation times ϕ_1 and ϕ_2, the TPA decay was fitted to the sum of two exponential terms:

$$r(t) = r_1 \exp^{-(t/\phi_1)} + r_2 \exp^{-(t/\phi_2)} + r_\infty \quad (3)$$

This method of analysis was established in our previous studies (*11, 15, 16*) and was validated by comparing residuals and χ^2 for fits with one, two and three exponential terms. As described previously, fits of the current data were optimal for $n = 2$ with residuals not exceeding 2% of the maximum anisotropy. The average correlation time $\langle\phi\rangle$ was calculated from

$$\langle\phi\rangle = (\phi_1 r_1 + \phi_2 r_2)/(r_1 + r_2) \quad (4)$$

Mass Spectrometry. The masses of monomeric actin were determined using a QSTAR quadrupole-TOF mass spectrometer (ABI) with an electrospray ionization source. Prior to infusion of actin, a solution of 50:50 acetonitrile:water and 0.1% formic acid (load solution) was infused at 50 μL per minute using an integrated syringe pump. After a stable, baseline total ion current (TIC) was established for the load solution, the protein (21 μM to 31 μM actin in G-buffer) was introduced into the solvent stream using a 10 μL injection loop installed in the integrated loop injector. After the TIC returned to baseline intensity, four more consecutive loop injections of the protein solution were made for a total of five injections per sample. Data were acquired continuously during load buffer infusion and protein infusions over the range 500−2000 m/z. The ESI spectra of actin were analyzed with BioAnalyst QS (ABI) software v 1.1.5. The Bayesian Protein Reconstruction tool was used to generate peak lists from the spectra, using a signal-to-noise threshold of twenty.

Interaction of S1 with Actin: Weak Binding Affinity and Actin-Activated ATPase. Biochemical experiments were performed using the same samples as the spectroscopic experiments. Weak binding affinity of S1 for actin was measured at 25 °C in Mg-F-buffer containing 3 mM ATP, and actin-activated S1 ATPase was measured at 25 °C in Mg-F-buffer containing 2.7 mM ATP, as described previously (*12, 13*). K_d was calculated by fitting the data to the equation $S1_b/S1_t = [A]/([A] + K_d)$, where $S1_b/S1_t$ is the fraction of S1 bound to actin, and [A] is the concentration of free actin. The extent of activation of fiber S1 ATPase by bulk muscle actin was measured at constant concentration of fiber S1 (0.9 μM) and increasing concentrations of actin, while the extent of activation of bulk muscle S1 by fiber actin was measured at constant concentration of actin (2.4 μM) and increasing concentrations of S1. These two experimental approaches were due to the limited amounts of proteins purified from fibers. V_{max} and K_m of acto-S1 ATPase were determined by fitting the data to the Michaelis−Menten equation using the software package Origin 7.0. Uncertainties of K_d, V_{max} and K_m were determined from statistical analysis of the fits.

Table 1: Interaction of Unoxidized and Oxidized S1 with ErIA-Actin in the Presence of ATP

S1	K_d, μM	V_{max}, s^{-1}	K_m, μM
unoxidized	5.33 ± 0.51	9.06 ± 0.34	4.18 ± 0.82
oxidized	4.89 ± 1.10	3.01 ± 0.07	1.39 ± 0.37

Statistical Analysis of Data. Each result is reported as mean ± SEM, unless indicated otherwise. The effects of oxidation were evaluated by one-way ANOVA, with Tukey posthoc tests performed for multiple comparisons. Differences were considered significant for $p < 0.05$.

RESULTS

Functional Interaction of Unoxidized and Oxidized S1 with ErIA-Actin. Oxidation of S1 decreased both V_{max} and K_m of acto-S1 ATPase by about a factor of 3, but the binding affinity (defined by K_d) was not affected (Table 1); these results are essentially the same as previously reported for unlabeled actin (*13*). The K_d of weak-binding affinity, about 5 μM (Table 1), was essentially the same as reported in our previous study using both ErIA-actin and myosin from unoxidized bulk muscle (*12*), and strong binding was stoichiometric, with K_d in the nanomolar range (data not shown). Thus we conclude that oxidation of S1 affects actin-activated ATPase activity but not actin affinity.

The effect of S1 Oxidation on Acto-S1 Dynamics. TPA decays in the absence of ATP (strong binding) show that strong binding of saturating amounts of S1 increased actin anisotropy, and the decays in the presence of saturating amounts of oxidized and unoxidized S1 were essentially the same (Figure 1, strong). Both the final anisotropy and the average correlation time (eq 4) were unaffected by oxidation ($p = 0.328$).

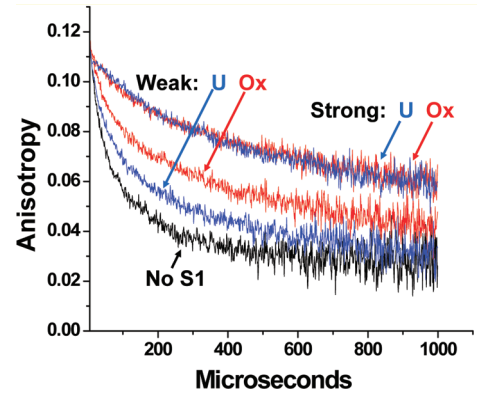

FIGURE 1: The effect of unoxidized (U) and oxidized (Ox) S1 (5 μM) on TPA of actin (1.2 μM) in the absence (strong) and the presence (weak) of ATP.

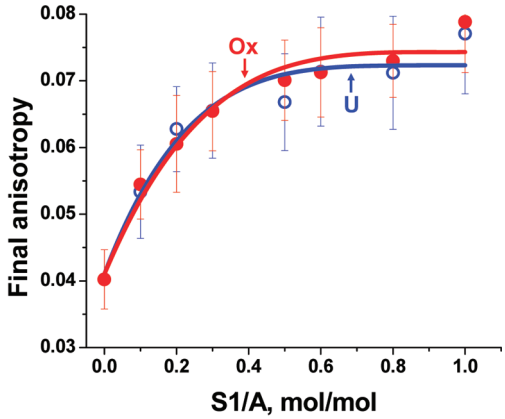

FIGURE 2: The effect of strongly bound unoxidized (opened symbols, U) and oxidized (closed symbols, Ox) S1 on the final anisotropy of actin. Fits to the linear lattice model (eq 2) are shown.

The effects of strongly bound S1 were analyzed in more detail by acquiring data as a function of S1/A and fitting the changes in the final anisotropy to the linear lattice model (Figure 2, eq 2). The resulting N values, corresponding to the number of monomers affected by one S1, were indistinguishable for S1 from oxidized ($N = 3.86 \pm 0.60$) and unoxidized ($N = 4.55 \pm 0.85$) fibers. Thus, we conclude that the functional (Table 1) and chemical (*13*) changes in myosin head induced by H_2O_2 treatment of fibers had no significant effect on the dynamics of strongly bound actin.

While S1 oxidation had no significant effect on the strongly bound complex, it had a substantial effect on the weakly bound complex, increasing the anisotropy and thus restricting the microsecond dynamics (flexibility) of actin (Figure 1). TPA decays of the weakly bound complexes were analyzed at two concentrations of added S1, 2.5 μM and 5 μM, which, according to the K_d of weak binding (Table 1), resulted in weak binding of 0.3 and 0.5 mol of S1/mol of actin, respectively. Both the final anisotropy and the correlation time were significantly ($p < 0.05$) higher (indicating decreased actin flexibility) due to S1 oxidation (Figure 3), and closer to the values obtained for the strongly bound complex. For example, in the presence of 0.5 mol of bound S1/mol of actin, the final anisotropy and correlation time of actin weakly bound to oxidized S1 (0.065 ± 0.002, $n = 48$, and 211 ± 8 μs, $n = 12$, respectively) were about 86% and 92%, respectively, of the final anisotropy and correlation time (0.076 ± 0.003, $n = 3$ and 231 ± 4 μs, $n = 3$) of strongly bound actin. In contrast, in the presence of the same amounts of bound unoxidized S1, the final anisotropy and correlation time (0.050 ± 0.002, $n = 48$ and 166 ± 4 μs, $n = 12$) of weakly bound actin were only about 68% and 69%, respectively, of the final anisotropy and correlation time (0.074 ± 0.004, $n = 3$ and 238 ± 23 μs, $n = 3$) of the strongly bound actin. Thus, oxidation-induced changes in S1 (*13*) significantly decreased the difference between the dynamics of weakly and strongly bound actin, decreasing the extent of the weak-to strong transition in actin dynamics.

The Effect of H_2O_2 Treatment of Fibers on the Properties of Actin. The yield of actin purified from fibers was similar in extracts from unoxidized (65 ± 12%) and oxidized fibers (64 ± 13%) (mean $\pm$ SD, $n = 4$). Incubation of purified actin with 3 mM $MgCl_2$ followed by 30 min centrifugation at 300000g pelleted about 96% of each actin sample. This

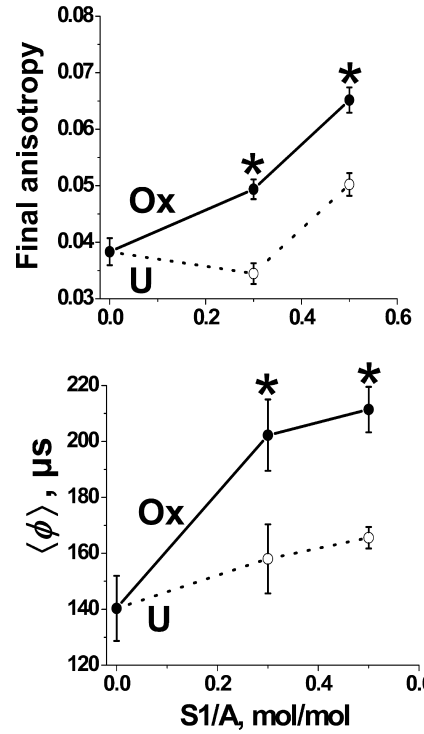

FIGURE 3: The effect of weakly bound unoxidized (U, opened symbols) and oxidized (Ox, closed symbols) S1 on the final anisotropy and the average correlation time $\langle\phi\rangle$ of actin. *: significantly different from unoxidized.

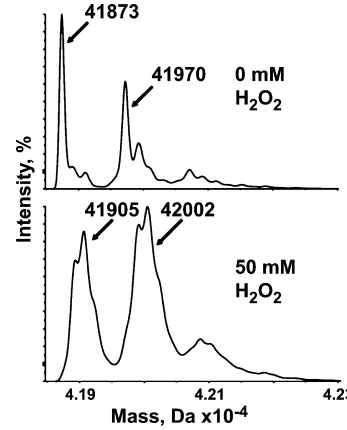

FIGURE 4: Mass profiles of actin purified from unoxidized and oxidized fibers.

shows that fiber oxidation did not affect the ability of actin to polymerize.

The MS spectrum of actin purified from unoxidized fibers (Figure 4, upper panel) showed a major mass peak of 41873.35 ± 1.64 Da (mean $\pm$ SD, $n = 2$), which corresponds to the predicted mass of skeletal muscle actin, 41872.29 Da (SwissProt primary accession number P68135). The second peak, with a mass of 41971.52 ± 1.00, was present in all our actin preparations (from fibers as well as from unoxidized skeletal muscle) in variable amounts and probably represents an ion adduct of the main peak. The MS spectrum of oxidized actin (Figure 4, lower panel) showed a clearly resolved mass peak of 41905.08 ± 1.72 Da, corresponding to a shift by 31.73 ± 0.09 Da from the mass of unoxidized actin. A similar shift, by 29.77 ± 4.41 Da, was detected for the ion adduct, indicating that it was susceptible to oxidization and therefore could not represent preoxidized actin species. The

Table 2: Interaction of Unoxidized and Oxidized Actin with S1 in the Presence of ATP

	unlabeled actin		ErIA-actin	
	unoxidized	oxidized	unoxidized	oxidized
K_d, μM	nd	nd	4.16 ± 0.92	5.13 ± 1.10
V_{max}, s^{-1}	17.32 ± 0.94	15.61 ± 0.86	11.20 ± 0.68	6.06 ± 0.25
K_m, μM	10.85 ± 1.28	14.90 ± 1.55	7.89 ± 1.23	3.84 ± 0.59

observed mass shift suggests the addition of two oxygen atoms. The MS spectrum of oxidized actin did not show a mass peak corresponding to unoxidized actin, indicating that essentially all actin was oxidized.

Functional Interaction of Unoxidized and Oxidized Actin with Muscle Myosin. Oxidation of actin did not have significant effect on the V_{max} of acto-S1 ATPase, however inhibitory effect was detected when oxidized and unoxidized actin were labeled with ErIA (Table 2). Since the extent of labeling was the same for oxidized and unoxidized actins (0.97 ± 0.09 and 0.97 ± 0.04 mol ErIA/mol actin, respectively), observed inhibition of the ATPase indicates that oxidation increased susceptibility of actin to probe-induced structural perturbations. In contrast to activation of myosin ATPase, the weak binding affinity of ErIA-labeled actin for S1 was not affected by actin oxidation (Table 2). Strong binding of ErIA-actin to myosin was also not affected by actin oxidation and was close to stoichiometric, with K_d in the nanomolar range (data not shown). Thus for both actin (Table 2) and S1 (Table 1) oxidation does not affect actomyosin affinity.

The Effect of Actin Oxidation on Acto-S1 Dynamics. In the absence of S1, TPA decays of ErIA-actin from oxidized and unoxidized fibers (Figure 5) did not show significant ($p \geq 0.11$) differences: the analysis of decays in terms of the sum of two exponential terms (eq 3) gave the initial anisotropy r_0 of 0.109 ± 0.002 and 0.108 ± 0.001, final anisotropy of 0.034 ± 0.002 and 0.035 ± 0.001 and average correlation time $\langle\phi\rangle$ of 116 ± 3 μs and 108 ± 4 μs (mean ± SEM, $n = 16$) for oxidized and unoxidized actin, respectively.

Oxidation of actin also had no significant effect on the final anisotropies of weakly or strongly bound actin ($p = 0.130$ and $p = 0.059$, respectively), and the 10% decrease in the average correlation time of weakly bound actin was not statistically significant ($p = 0.12$) (Figure 6). Oxidation decreased the correlation time of strongly bound actin, and in this case the 20% decrease (from 128 ± 8 μs to 99 ± 6 μs) was statistically significant ($p = 0.002$, $n = 18$) (Figure 6). However, there was not a significant effect of actin oxidation on the difference between weak and strong, as measured by final anisotropy or correlation time.

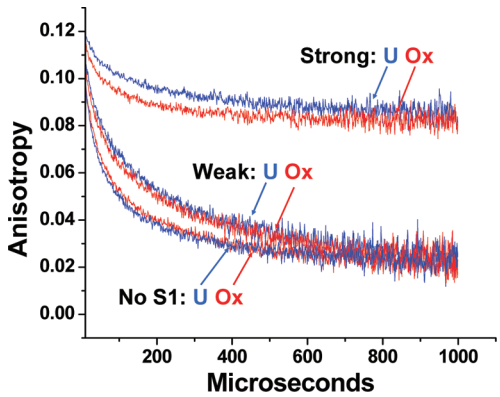

FIGURE 5: The effect of weakly and strongly bound S1 on TPA of unoxidized (U) and oxidized (Ox) actin.

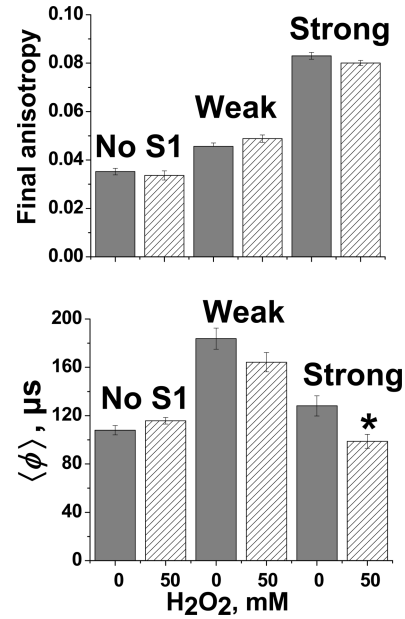

FIGURE 6: The effect of weakly and strongly bound S1 on the final anisotropy and the average correlation time $\langle\phi\rangle$ of unoxidized (filled bars) and oxidized (hatched bars) actin (1.2 μM). S1 bound per mole of actin: weak, 0.3; strong, 1. *: significantly different from unoxidized.

Cumulative effects of oxidation of both actin and myosin were determined using actomyosin complexes containing both actin and myosin either from unoxidized or oxidized fibers. The results showed that the final anisotropy and correlation time of the strongly bound oxidized complex (0.078 ± 0.006) were essentially the same as those of strongly bound unoxidized complex (0.077 ± 0.004, mean ± SD, $n = 2$). In the weakly bound complexes, final anisotropy of actin in the oxidized complex (0.059 ± 0.001) was about 45% higher than that of actin in the unoxidized complex (0.041 ± 0.001) (mean ± SEM, $n = 24$), and the average correlation time of actin in the oxidized complex (209 ± 10 μs) was about 33% higher than that in the unoxidized complex (157 ± 7 μs) (mean ± SEM, $n = 8-10$). Thus, oxidation of both actin and myosin produced essentially the same result as oxidation of myosin alone (Figures 2 and 3).

DISCUSSION

Summary. We report that peroxide-induced inhibition of muscle contractility and actomyosin ATPase activity is associated with changes in the extent of the weak-to-strong structural transition in actin dynamics. Oxidation of myosin has the predominant effect, which is to decrease the flexibility of actin in the weakly bound complex (Figure 1). The net result is to decrease the amplitude of the dynamic disorder-to-order transition in actin dynamics that occurs in the W-to-S transition. This change in actin dynamics is complementary to the previously reported peroxide-induced decrease in the magnitude of the disorder-to-order transition in myosin dynamics in the same muscle (*13*). We conclude that dynamic disorder-to-order transitions in both actin and myosin are coupled and are essential for the enzymatic and contractile function of muscle.

The Effect of S1 Oxidation on Structural Transitions in Actin. Previous studies on peroxide-treated muscle fibers used myosin-specific EPR to show that structural states of myosin under rigor and contraction conditions were not significantly affected by peroxide treatment, but peroxide had a significant effect on relaxation conditions, increasing the fraction of myosin in the strongly bound structural state from 0 to 34% (*13*). Corresponding structural changes in actin could not be analyzed within muscle fibers, so these are analyzed in the present study using purified proteins. Oxidation of S1 restricts the rotational dynamics of weakly bound actin, decreasing the difference between the weak and strong complexes (Figures 1, 2, and 3). A possible explanation for this shift is that the increased rigor-like structural state of myosin heads in oxidized fibers (*13*) is preserved in purified S1. Thus, we conclude that the oxidation-induced decrease in the weak-to-strong transition in myosin S1 is coupled to a parallel decrease in the weak-to-strong transition in actin.

Previous evidence for the functional coupling of weak-to-strong structural transitions in both actin and myosin came mainly from nucleotide-dependent changes in myosin, which probably act by altering the structure of the weak and strong actin−myosin interface (*1, 7, 9, 12, 17*). The effects of oxidation-induced changes in myosin on the dynamics of actin (Figure 3) are also probably related to changes at the interface, as suggested by decreased enzymatic activity of actomyosin in the presence of oxidized S1 (Table 1). These changes could be induced directly by the proposed oxidation of sites located at the interface, and/or induced allosterically by oxidation of other myosin sites (*13*). The molecular mechanism of structural coupling between actin and myosin probably involves shifts among structural states of actin, analogous to proposed shifts in response to binding of various proteins (*18, 19*). Our previous studies on the role of actin dynamics in the function of actomyosin led to the hypothesis that stabilization of actin in a strongly bound structural state in the absence of myosin inhibits structural transitions required for function of actomyosin (*11, 15*). The present study suggests that functionally important structural transitions in actin can be also inhibited by stabilizing actin in specific structural states during weak interactions with myosin.

The Effect of H_2O_2 Treatment of Muscle on Actin. Mass spectrometry showed that H_2O_2 treatment of fibers resulted in oxidative modifications of actin by addition of two oxygen atoms (Figure 4). Peroxide treatment of actin was studied previously, but those studies were performed on monomeric actin in solution and indicated that oxidation can affect at least six sites with significant destabilizing effects on the structure of actin monomer and filament (*20*). Since that study did not analyze modification quantitatively, we compared the effect of oxidation of actin in fibers and in solution using mass spectrometry. The analysis of the effects of hydrogen peroxide treatment of purified skeletal muscle G-actin in solution under the same conditions as applied for fibers (50 mM H_2O_2, 30 min treatment at 25 °C) showed that oxidation increased the mass of the purified actin by 66.73 ± 3.44 Da, indicating addition of four oxygen atoms. Thus, the extent of H_2O_2 oxidation of purified actin is higher than that of actin oxidized within muscle fibers (Figure 4). This result suggests a protective effect of the muscle filament lattice and justifies caution in extrapolating results obtained by oxidation of purified muscle proteins to results obtained by oxidation of the same proteins in muscle.

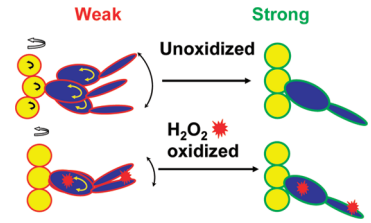

FIGURE 7: Schematic of oxidation-induced changes in structural transitions in actin and myosin.

While specific oxidation sites were not determined in this study, it is unlikely that they include Cys374, since reactivity of fiber actin with the Cys374-specific probe ErIA (*10*) was unaffected by oxidation. The oxidized sites probably include some of the methionines indentified in peroxide-treated purified skeletal muscle G-actin (*20, 21*); methionines have been also previously proposed as most likely targets of H_2O_2 oxidation in myosin from the same fibers (*13*).

Oxidation of actin in muscle fibers had no significant effect on the dynamics of actin filaments (Figure 5). Although the dynamics was measured using phalloidin-stabilized actin, control experiments using phalloidin-free actin also did not detect significant differences between the dynamics of unoxidized and oxidized actin, as indicated by similarity of their normalized final anisotropies ($r_{400-500}/r_0$), 0.230 ± 0.027 and 0.211 ± 0.01 (mean ± SD, $n = 3$), respectively. Thus, under our experimental conditions, phalloidin did not attenuate the effects of oxidation on actin dynamics. The stabilization of actin by phalloidin (*22*) in the presented spectroscopic and functional measurements was critical, since multiple control experiments showed that at pH >7.0 phalloidin-free ErIA-actin filaments are unstable and show time-dependent depolymerization and/or denaturation. The lack of significant effect of oxidation on actin dynamics (Figure 6) contrasts our previous findings where perturbations of actin by cross-linkers and site-specific mutations had substantial effects (*11, 15, 16*). This suggests that the molecular mechanism of perturbation-induced changes in the dynamics of actin is specifically dependent on the affected regions.

The dynamics of actin in the presence of S1 showed that oxidation affected the dynamics of the strongly bound complex, but these changes were too small to have significant effect on the extent of weak-to-strong transitions (Figure 6). Since structural effects of actin oxidation could be detected only after ErIA labeling, and this significantly enhanced functional effects of oxidation (Table 2), it is likely that dynamics of unlabeled actin in the presence of strongly and weakly S1 was not affected by oxidation. Thus, we concluded that the effects of oxidation on the dynamics of actin in the actomyosin complex are predominantly determined by oxidation-induced changes in myosin S1.

In summary, our results provide clear evidence of coupling between structural transitions in actin and myosin during the actomyosin ATPase cycle (Figure 7). We conclude that the molecular mechanism of oxidation-induced inhibition of muscle contractility and enzymatic activity is associated with decreased amplitude of dynamic disorder-to-order transitions in both actin and myosin, during the weak-to-strong transition in the actomyosin ATPase cycle. These

results provide insight into the functional basis of actomyosin structural dynamics, with particular relevance to the effects of oxidative stress in muscle (*13*), which increases with aging and disease (*5*).

ACKNOWLEDGMENT

The authors thank Deborah Ferrington and LaDora Ferrington for discussion of the manuscript, Leanne Kolb for preparation of skinned muscle fibers, LeeAnn Higgins for assistance in analysis of mass spectrometry data, Octavian Cornea for assistance with preparation of the manuscript and the Minnesota Supercomputing Institute for computational resources. The mass spectrometric measurements were performed at the Center for Mass Spectrometry and Proteomics.

REFERENCES

1. Rayment, I., Holden, H. M., Whittaker, M., Yohn, C. B., Lorenz, M., Holmes, K. C., and Milligan, R. A. (1993) Structure of the actin-myosin complex and its implications for muscle contraction. *Science 261*, 58–65.
2. Thomas, D. D., Ramachandran, S., Roopnarine, O., Hayden, D. W., and Ostap, E. M. (1995) The mechanism of force generation in myosin: a disorder-to-order transition, coupled to internal structural changes. *Biophys. J. 68*, 135S–141S.
3. Thomas, D. D., Prochniewicz, E., and Roopnarine, O. (2002) Changes in actin and myosin structural dynamics due to their weak and strong interactions. *Results Probl. Cell Differ. 36*, 7–19.
4. Lowe, D. A., Surek, J. T., Thomas, D. D., and Thompson, L. V. (2001) Electron paramagnetic resonance reveals age-related myosin structural changes in rat skeletal muscle fibers. *Am. J. Physiol.: Cell Physiol. 280*, C540–547.
5. Prochniewicz, E., Thompson, L. V., and Thomas, D. D. (2007) Age-related decline in actomyosin structure and function. *Exp. Gerontol. 42*, 931–938.
6. Ng, C. M., and Ludescher, R. D. (1994) Microsecond rotational dynamics of F-actin in ActoS1 filaments during ATP hydrolysis. *Biochemistry 33*, 9098–9104.
7. Yanagida, T., Nakase, M., Nishiyama, K., and Oosawa, F. (1984) Direct observation of motion of single F-actin filaments in the presence of myosin. *Nature 307*, 58–60.
8. Prochniewicz-Nakayama, E., Yanagida, T., and Oosawa, F. (1983) Studies on conformation of F-actin in muscle fibers in the relaxed state, rigor, and during contraction using fluorescent phalloidin. *J. Cell Biol. 97*, 1663–1667.
9. Borovikov, Y. S., Dedova, I. V., dos Remedios, C. G., Vikhoreva, N. N., Vikhorev, P. G., Avrova, S. V., Hazlett, T. L., and Van Der Meer, B. W. (2004) Fluorescence depolarization of actin filaments in reconstructed myofibers: the effect of S1 or pPDM-S1 on movements of distinct areas of actin. *Biophys. J. 86*, 3020–3029.
10. Prochniewicz, E., Zhang, Q., Howard, E. C., and Thomas, D. D. (1996) Microsecond rotational dynamics of actin: spectroscopic detection and theoretical simulation. *J. Mol. Biol. 255*, 446–457.
11. Prochniewicz, E., and Thomas, D. D. (1997) Perturbations of functional interactions with myosin induce long-range allosteric and cooperative structural changes in actin. *Biochemistry 36*, 12845–12853.
12. Prochniewicz, E., Walseth, T. F., and Thomas, D. D. (2004) Structural dynamics of actin during active interaction with myosin: different effects of weakly and strongly bound myosin heads. *Biochemistry 43*, 10642–10652.
13. Prochniewicz, E., Lowe, D. A., Spakowicz, D., Higgins, L. A., Thompson, L. T., Ferrington, D. A., and Thomas, D. D. Functional, structural and chemical changes in myosin associated with hydrogen peroxide treatment of skeletal muscle fibers, *Am. J. Physiol.: Cell Physiol.*, submitted.
14. Bradford, M. M. (1976) A Rapid and Sensitive Method for the Quantitation of Microgram Quantities of Protein Utilizing the Principle of Protein-Dye Binding. *Anal. Biochem. 72*, 248–254.
15. Prochniewicz, E., and Thomas, D. D. (2001) Site-specific mutations in the myosin binding sites of actin affect structural transitions that control myosin binding. *Biochemistry 40*, 13933–13940.
16. Prochniewicz, E., and Thomas, D. D. (1999) Differences in structural dynamics of muscle and yeast actin accompany differences in functional interactions with myosin. *Biochemistry 38*, 14860–14867.
17. Andreev, O. A., and Reshetnyak, Y. K. (2007) Mechanism of formation of actomyosin interface. *J. Mol. Biol. 365*, 551–554.
18. Galkin, V. E., Orlova, A., Lukoyanova, N., Wriggers, W., and Egelman, E. H. (2001) Actin depolymerizing factor stabilizes an existing state of F-actin and can change the tilt of F-actin subunits. *J. Cell Biol. 153*, 75–86.
19. Prochniewicz, E., Janson, N., Thomas, D. D., and De la Cruz, E. M. (2005) Cofilin increases the torsional flexibility and dynamics of actin filaments. *J. Mol. Biol. 353*, 990–1000.
20. Milzani, A., Rossi, R., Di Simplicio, P., Giustarini, D., Colombo, R., and DalleDonne, I. (2000) The oxidation produced by hydrogen peroxide on Ca-ATP-G-actin. *Protein Sci. 9*, 1774–1782.
21. Milzani, A., DalleDonne, I., and Colombo, R. (1997) Prolonged oxidative stress on actin. *Arch. Biochem. Biophys. 339*, 267–274.
22. Estes, J. E., Selden, L. A., and Gershman, L. C. (1981) Mechanism of action of phalloidin on the polymerization of muscle actin. *Biochemistry 20*, 708–712.

BI801080X